AD NUMBER

AD261501

NEW LIMITATION CHANGE

TO

Approved for public release, distribution unlimited

FROM

Distribution authorized to U.S. Gov't. agencies and their contractors; Operational and administrative use; Aug 1961. Other requests shall be referred to Arnold Engineering Development Center, TN.

AUTHORITY

AEDC ltr, 7 Jun 2002

AEDC-TN-61-96

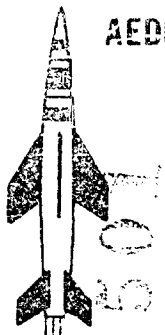

PRESSURE DISTRIBUTIONS ON A HEMISPHERE CYLINDER AT SUPERSONIC AND HYPERSONIC MACH NUMBERS

By

A. L. Baer

VKF, ARO, Inc.

August 1961

ARNOLD ENGINEERING DEVELOPMENT CENTER

AIR FORCE SYSTEMS COMMAND

U S A F

PRESSURE DISTRIBUTIONS ON A HEMISPHERE CYLINDER AT SUPERSONIC AND HYPERSONIC MACH NUMBERS

By

A. L. Baer

VKF, ARO, Inc.

August 1961

ARO Project No. 300116

Contract No. AF 40(600)-800 S/A 24(61-73)

Program Area 750A, AFSC Project No. 8952, Task No. 89512

ABSTRACT

Pressure distribution tests at supersonic and hypersonic speeds were conducted in the von Karman Gas Dynamics Facility (VKF), Arnold Center, Air Force Systems Command on AGARD Model E, a hemisphere cylinder configuration.

Various experimental data concerning the aerodynamic characteristics of blunt nosed bodies are available; however, relatively few sources present findings over a wide Mach number range. The present investigations, stimulated by the need for applicable experimental data to compare with the predictions of various theories, were conducted at Mach numbers 2 through 8 over a Reynolds number range from 0.17×10^6 to 0.51×10^6 per inch.

This report presents a comparison of experimental results with available theoretical predictions of pressure distributions, pressure drag, shock wave shapes, and bow shock wave detachment distances.

CONTENTS

TABLES

ILLUSTRATIONS

NOMENCLATURE

C_{D_p}	Pressure drag coefficient, $\int_0^1 C_p \, d(r/r_o)^2$
C_p	Pressure coefficient, $\frac{p_x - p_\infty}{q_\infty}$
$C_{p_{max}}$	Pressure coefficient at stagnation point
d	Model diameter, in.
M_∞	Free-stream Mach number
p_o	Stilling chamber pressure, psia
p_x	Local static pressure, psia
p_∞	Free-stream static pressure, psia
q_∞	Free-stream dynamic pressure, psia
r	Orifice coordinate defined by Fig. 3, in.
r_o	Hemispherical nose radius, in.
R	Shock wave coordinate defined by Fig. 3, in.
Re	Reynolds number
T_o	Stilling chamber temperature, °R
x	Distance in axial direction measured from forward stagnation point, in.
δ	Detachment distance of bow shock wave, in.
θ	Angular dimension on hemispherical nose measured with respect to the model axial centerline, deg
γ	Ratio of specific heats for air

INTRODUCTION

In support of present day trends toward blunted aerodynamic shapes for supersonic and hypersonic speeds, various approximations have been developed to describe the flow characteristics about bodies with blunted leading edges. Certain theories are widely known and accepted for use in the derivation of pressure distributions and pressure drag coefficients over spheres and other blunt shapes, while other approximations deal with shock wave shapes and bow shock wave detachment distances. There is, however, a shortage of applicable experimental data which in turn precludes a comparison of theoretical methods with empirical results to determine which theoretical procedures best predict the characteristics of blunt-nose bodies. A test program was initiated to provide experimental data for comparison with theoretical predictions of pressure distributions, pressure drag, shock wave shapes, and bow shock wave detachment distances as applied to the axisymmetric blunt body problem.

Tests were conducted on AGARD Model E in the VKF 40 by 40-inch supersonic wind tunnel (Tunnel A) and in the 50-inch-diam hypersonic tunnel (Tunnel B) at the Arnold Engineering Development Center. Pressure distribution and bow shock wave shapes were obtained at Mach numbers 2, 3, 4, 5, 6, and 8 at zero angle of attack. Reynolds numbers for these tests varied from 0.17×10^6 to 0.51×10^6 per inch.

A comparison of experimental results of pressure distributions, pressure drag, shock wave shapes, and bow shock wave detachment distances with the predictions of various theories are presented in this report.

APPARATUS

WIND TUNNELS

The 40 by 40-in. tunnel (Tunnel A) shown in Fig. 1 is a continuous, closed circuit, variable density, supersonic wind tunnel with a Mach number range from 1.5 to 6. Variations in Mach number are produced with flexible plates which are automatically positioned at the desired contour by electrically driven jack units. A complete description of Tunnel A may be found in Ref. 1.

Manuscript released by author July 1961.

Tunnel B (Fig. 2) is an axisymmetric, continuous-flow, variable density, hypersonic wind tunnel with a 50-in. -diam test section. Because of changes in boundary-layer thickness due to changing pressure level, the Mach 8 contoured nozzle produces an average test section Mach number which varies from 8.02 at a stagnation pressure of 100 psia to 8.10 at 800 psia. The centerline flow distribution is uniform within ±1 percent in Mach number, whereas off-center the flow is uniform to about ±0.3 percent. There is a slight axial gradient on the order of 0.01 Mach number per foot.

The continuous tunnels at the von Karman Gas Dynamics Facility are driven by a 100,000-hp central compressor system arranged to provide a total of nine stages of compression. For operation of Tunnel A, up to five stages of compression are utilized to provide a Reynolds number range from 0.3×10^6 to 9.0×10^6 per ft at $M_\infty = 1.5$ and from 0.4×10^6 to 4.3×10^6 at $M_\infty = 6$. Variable densities are obtained at each Mach number by introducing air from a 5300-cu-ft, 4000-psia storage system. Below Mach number 4, the tunnel is operated at stagnation temperatures of approximately 100°F, whereas for tests at the higher Mach numbers, this temperature can be raised to a maximum of 300°F to prevent test section air liquefaction. Supply air is processed through large capacity, silica-gel driers to maintain an absolute humidity below 0.0001 lb of water per lb of air (dew point of -35°F at atmospheric pressure).

Stagnation pressures up to approximately 800 psia are supplied to Tunnel B by the compressor system. A propane fired heater produces a maximum air temperature of 900°F, sufficient to prevent liquefaction of the air in the test section.

MODEL

The model (Figs. 3 and 4), designed and built by the VKF, consisted of two sections: (1) a cylindrical body 5.80 in. in diameter and 31.55 in. long, and (2) a hemispherical nose section of 2.90-in. radius, 7.60 in. long. The overall model was 6.75 body diameters or 39.15 in. long.

The model was instrumented with 28 pressure orifices arranged in a single ray along the body from the stagnation point. The hemispherical portion of the nose section contained 10 orifices spaced at 10-deg intervals from the stagnation orifice. Three additional orifices on the nose section were equally spaced beginning at 1 in. from the shoulder orifice. The pressure orifice arrangement on the cylindrical

body section began 0.625 in. beyond the nose-body joint, and orifices were equally spaced at 2-in. intervals to within approximately one-half of a body diameter of the model base.

INSTRUMENTATION AND PRECISION OF RESULTS

Model pressures in Tunnel A were measured with a system of 15-, 5-, and 1-psid transducers connected to orifices along the body in such a manner as to give the desired sensitivity depending upon orifice location. These transducers will record pressures to a precision of approximately 0.1 percent of the rated capacity.

In Tunnel B, model pressures were measured with a sequential pressure switching system having nine synchronized valves, each valve being connected to a 5-psid transducer. To attain various ranges of instrument sensitivity, seven reference pressures which could be varied in approximately 2-psia increments from a near vacuum were available. Each transducer was calibrated for a range of ±0.3, ±0.6, and ±1.2 psid, and these ranges, in conjunction with the seven reference pressures, were automatically selected to insure the best available precision of pressure measurement.

The pressure distribution data presented in this report are subject to the following uncertainties based on repeatability of measurements:

Nominal M_∞	p_x/p_∞
2	±0.010
3	±0.010
4	±0.015
5	±0.025
6	±0.050
8	±0.050

TEST PROCEDURE

The conditions at which these tests were conducted are summarized in the table on the following page:

Nominal M_∞	p_o, psia	T_o, °R	$Re \times 10^{-6}$, per inch
2	8.1	555	0.17
3	32.3	605	0.35
4	71.9	623	0.44
5	150.7	655	0.51
6	174.5	683	0.37
	174.8	738	0.33
8	650	1340	0.22

All data presented were obtained at zero angle of attack and zero-deg roll angle.

Photographs to define the shock wave shape at supersonic Mach numbers were made with a double-pass schlieren system and a shadowgraph system which was utilized strictly for photographs of the nose region (see Fig. 5). In Tunnel B, a conventional, short-range, divergent ray, spark shadowgraph system was used to record flow patterns about the nose of the model.

RESULTS AND DISCUSSION

NOSE PRESSURE DISTRIBUTIONS

Pressure distributions over the hemispherical nose of AGARD Model E at all test Mach numbers, as given in Table 1, are presented in Fig. 6 along with other $M_\infty = 6$ data obtained in the VKF (Ref. 2) and certain results at Mach numbers 1.97 and 3.04 by Perkins and Jorgensen as presented in Ref. 3. Theoretical comparisons to the experimental data in the form p_x/p_∞ are afforded by the modified Newtonian approximation ($C_p = C_{p_{max}} \cos^2\theta$) and by the solutions of Van Dyke and Gordon for a sphere with $\gamma = 1.4$ (Ref. 4). In addition, the experimental results are compared with a prediction of the local pressure ratio obtained by the following empirical expression for local pressure coefficient (Ref. 3).

$$C_p = 2\cos^2\theta - \left(2 - C_{p_{max}}\right)\cos\theta \qquad (1)$$

The modified Newtonian approximation has long been known to give satisfactory predictions within certain restrictions, and, except for the results at $M_\infty = 6$ and 8, good agreement is shown here until the nose-cylinder junction is approached. The solution at the shoulder ($\theta = 90$ deg) gives $p_x = p_\infty$ which is generally valid only for the lower

Mach numbers. By matching the Newtonian approximation with the Prandtl-Meyer relation at the point on the surface where both the pressure and the pressure gradient given by the two formulas are equal, the pressure distribution may be predicted to the shoulder. For the present comparisons, this approach was used for M_∞ = 6 and 8 and is in excellent agreement with the experimental results.

The methods of Ref. 4 which, for a sphere, results in the "Newtonian plus centrifugal" analytic approach of Busemann, also show excellent agreement with experimental points. These predictions, as stated by Van Dyke and Gordon, do not extend to θ = 60 deg where the Newtonian theory plus centrifugal force effects results in the pressure at the surface being zero ($p_x = 1 - 4/3 \sin^2 \theta$).

It should be noted that the solutions presented in Ref. 4 were obtained for what herein are called nominal Mach numbers. These solutions were used strictly as given by shifting the ordinate to correspond with the theoretical p_x/p_∞ depending on the calibrated Mach number. Also, the predictions for M_∞ = 8.10 required an interpolation between Mach numbers 6 and 10, which apparently was satisfactory.

To obtain the empirical expression given in Ref. 3 for the pressure distribution, the assumption was made that the expansion of the flow over the hemisphere is similar to that predicted by Newtonian theory but differs from theory by an amount which varies approximately as the cosine of the angle θ. The approximation provides results which agree well with experimental findings but, like the Newtonian theory at high Mach numbers, is inadequate as the shoulder is approached.

PRESSURE DISTRIBUTIONS ALONG THE CYLINDER

Table 2 gives the experimental pressure distributions along the cylindrical body, and these results are compared with the theoretical methods of Love (Ref. 5) in Fig. 7. The method of Ref. 5 for $M_\infty \gg 1$ may be taken as a modification of blast wave theory since the blast wave pressure decay laws were utilized. Love has suggested the use of the experimental shoulder pressure to bring the predicted pressure distributions into closer agreement with experimental values. This was done for all test Mach numbers with the difference between the purely theoretical and the "theoretical plus experimental" approaches being shown for M_∞ = 6.02. It is interesting to note that for M_∞ = 8.10 the shoulder pressure was exactly as predicted by Love, and modifications were not needed.

The approximate solutions, based on blast analogy, of inviscid, hypersonic flows about simple slender bodies as suggested by J. Lukasiewicz in Ref. 6 were also used for pressure distribution comparisons at M_∞ = 5.06, 6.02, and 8.10. To use the methods of Ref. 6 (γ = 1.4), one must know, in addition to M_∞, the drag coefficient which defines the flow field. For the comparisons shown, the drag coefficients used were the experimentally determined values of C_{D_p} at the appropriate Mach numbers. Here one should note that the second approximation for the pressure distribution (axisymmetric flow) given by Ref. 6 greatly improves the predictions afforded by the first approximation, and although deficiencies exist near the shoulder region, agreement with experimental data improves in the aft region of the body.

PRESSURE DRAG

A comparison between experimental pressure drag coefficients and values determined with the modified Newtonian approximation are presented in Table 3 and shown in Fig. 8. The theoretical values are slightly higher than the experimental results as would be expected since the modified Newtonian pressure distributions presented in Fig. 6 are higher than the experimental results; specifically for θ values between 20 and 60 deg where the section loading is high as opposed to beyond 60 deg. Here the local surface slope is small and will not result in an appreciable change in pressure drag even though there exists in some cases large differences between the theoretical predictions and experimental results (see Fig. 6, M_∞ = 6.03 and 8.10).

It was shown in Ref. 3 that the pressure distributions follow closely an empirical relation (see Eq. 1) which results in the expression, $C_{D_p} = \frac{2\,C_{p_{max}} - 1}{3}$. Pressure drag values determined in this manner agree well with the majority of the experimental data presented in Fig. 8.

SHOCK WAVE SHAPE

The experimental shock wave shape coordinates given in Table 4 were obtained from scaling schlieren photographs similar to Fig. 5a. Figure 9 presents a comparison between these experimental shock wave shapes and the theoretical shapes obtained by the methods of Ref. 11. Excellent agreement with experimental results is shown for Mach numbers 1.99, 3, and 4.03, whereas small deviations exist for the higher Mach numbers. The first and second approximations for shock wave

shape as given by blast analogy (Ref. 6) are included for comparisons at Mach numbers 5.06 and 6.03. Here one should note that although the experimental shock wave is displaced from the body more than predicted by blast analogy, the second approximation affords predictions of shock wave slope.

BOW SHOCK WAVE DETACHMENT DISTANCE

Bow shock wave detachment distances at all test Mach numbers were obtained from measurements of photographs similar to Fig. 5b and are presented in Fig. 10. The methods of Ref. 11, which were used for predicting shock wave shapes show excellent agreement with empirical bow shock wave detachment distances. The theory presented in Ref. 4 also gives satisfactory results. All of these theoretical predictions, excluding Ref. 12, for Mach numbers above 4 predict detachment distances greater than experimentally determined values.

CONCLUDING REMARKS

Tests were conducted at Mach numbers 2 through 8 at zero angle of attack to obtain pressure distribution and optical data on AGARD Model E for comparison with theoretical predictions of pressure distribution, pressure drag coefficients, shock wave shapes, and bow shock wave detachment distances. The results of these investigations indicate that:

1. Excellent agreement with theory in the shoulder region was obtained at Mach numbers above 5 by matching the Newtonian approximation with the Prandtl-Meyer relation at the point on the surface where the pressure gradient and pressure given by the two relationships are equal.
2. The modified Newtonian approximation generally overestimated the pressure distribution but when modified by an empirical relation from Ref. 3 agreed well with experimental results.
3. Pressure distributions over a hemisphere can be closely predicted by the methods of Ref. 4 for θ less than 40 deg.
4. Along the cylindrical body downstream of the hemispherical nose, the methods presented by Ref. 5 do not give satisfactory predictions of the pressure distribution.

5. Pressure drag coefficients for a hemisphere are overestimated using the modified Newtonian approximation but agree well with an empirical relation given in Ref. 3.
6. The methods of Ref. 11 afford a good prediction of shock wave shapes for the hemisphere-cylinder model.
7. References 11 and 4 give a good approximation of bow shock wave detachment distances.

REFERENCES

1. Schueler, C. J. and Strike, W. T. "Calibration of a 40-Inch Continuous Flow Tunnel at Mach Numbers 1.5 to 6." AEDC-TN-59-136, November 1959.
2. VKF-AEDC Investigations of a Spherically Blunted Cone at Mach Number 6.
3. Perkins, E. W. and Jorgensen, L. H. "Investigation of the Drag of Various Axially Symmetric Nose Shapes of Fineness Ratio 3 for Mach Numbers from 1.24 to 3.67." NACA-RM-A52H28, November 1952.
4. Van Dyke, M. D. and Gordon, H. D. "Supersonic Flow Past a Family of Blunt Axisymmetric Bodies." NASA Technical Report R-1, 1959.
5. Love, E. S. "Prediction of Inviscid Induced Pressures from Round Leading Edge Blunting at Hypersonic Speeds." ARS Journal, Vol. 29, October 1959, pp. 792 - 794.
6. Lukasiewicz, J. "Hypersonic Flow-Blast Analogy." AEDC-TR-61-4, June 1961.
7. Sommer, S. C. and Stark, J. A. "The Effect of Bluntness on the Drag of Spherically Tipped Truncated Cones of Fineness Ratio 3 at Mach Numbers 1.2 to 7.4." NACA-RM-A52B13, April 1952.
8. Chauvin, L. T. "Pressure Distribution and Pressure Drag for a Hemispherical Nose at Mach Numbers 2.05, 2.54, and 3.04." NACA-RM-L52K06, December 1952.
9. Hunt, G. K. "Supersonic Wind Tunnel Study of Reducing the Drag of a Bluff Body at Incidence by Means of a Spike." RAE Report No. AERO 2606, May 1958.

10. Beecham, L. J. "The Hemispherical, Differential Pressure Yawmeter at Supersonic Speeds." RAE Technical Note No. AERO 2687, June 1960.

11. Love, E. S. "A Re-examination of the Use of Simple Concepts for Predicting the Shape and Location of Detached Shock Waves." NACA-TN-4170, December 1957.

12. Stollery, J. L. and Maull, D. J. "A Note on Shock Detachment Distance." Journal of the Royal Aeronautical Society. Vol. 64, June 1960, p. 357.

13. Serbin, Hyman. "Supersonic Flow around Blunt Bodies." Readers' Forum, Journal of the Aeronautical Sciences, Vol. 25, No. 1, January 1958, p. 58.

TABLE 1
VARIATION OF p_x/p_∞ WITH HEMISPHERICAL NOSE ANGLE θ

	M_∞	1.99	3.00	4.03	5.06	6.02	6.03	8.10
	Re/in. x 10^{-6}	0.17	0.35	0.44	0.51	0.33	0.37	0.22
Orifice No.	Nose Angle θ deg							
1	0	5.598	12.07	21.35	33.56	-	47.43	-
2	10	5.433	11.63	20.54	32.29	45.65	45.67	83.45
3	20	5.006	10.55	18.50	28.87	-	40.98	73.03
4	30	4.319	8.879	15.39	23.93	-	33.89	60.74
5	40	3.568	7.075	12.09	18.70	-	26.39	46.61
6	50	2.759	5.214	8.702	13.29	18.44	18.72	32.84
7	60	2.073	3.646	5.911	8.909	12.52	12.52	21.51
8	70	1.437	2.349	3.686	5.396	7.428	7.564	12.96
9	80	0.9549	1.409	2.135	3.051	4.237	4.252	7.230
10	90	0.6282	0.8303	1.238	1.698	2.262	2.341	3.823

TABLE 2
VARIATION OF p_x/p_∞ WITH DISTANCE DOWNSTREAM OF THE SHOULDER POINT

	M_∞	1.99	3.00	4.03	5.06	6.02	6.03	8.10
	Re/in. x 10^{-6}	0.17	0.35	0.44	0.51	0.33	0.37	0.22
Orifice No.	x/d							
10	0.5000	0.6282	0.8303	1.238	1.698	2.262	2.341	3.823
11	0.6724	0.6929	0.8072	1.159	1.516	2.022	2.035	3.277
12	0.8448	0.7503	0.8241	1.132	1.452	-	-	3.066
13	1.0173	0.7919	0.8452	1.113	1.386	1.916	1.874	-
14	1.4182	0.8359	0.8623	1.020	1.251	1.729	1.743	2.505
15	1.7630	0.8768	0.8747	0.9892	1.193	-	1.605	2.247
16	2.1079	0.9111	0.8809	0.9446	1.122	-	1.503	2.052
17	2.4527	0.9475	0.8800	0.9257	1.061	1.333	1.386	1.891
18	2.7975	-	0.8706	-	-	-	-	1.754
19	3.1424	1.014	0.8681	0.8789	0.9535	1.169	1.219	1.657
20	3.4872	1.042	0.8705	0.8707	0.9299	1.107	1.182	1.557
21	3.8320	-	0.8713	-	-	1.065	-	1.472
22	4.1768	1.015	0.8561	0.8621	0.8788	-	-	1.407
23	4.5217	1.038	0.8927	-	-	-	-	1.374
24	4.8665	1.009	0.8898	0.8594	0.8765	1.039	1.124	1.336
25	5.2113	1.019	0.9008	0.8687	0.8677	1.019	1.117	1.286
26	5.5562	1.031	0.9314	0.8899	0.8677	-	1.113	-
27	5.9010	1.018	0.9127	0.8865	0.8595	1.015	1.101	1.147
28	6.2458	1.021	0.9200	0.8982	0.8548	1.013	1.080	1.149

TABLE 3
COMPARISON OF EXPERIMENTAL PRESSURE DRAG COEFFICIENTS
TO MODIFIED NEWTONIAN PRESSURE DRAG COEFFICIENTS

M_∞	$1/M_\infty^2$	Re/in. x 10^{-6}	C_{D_p} Experimental	C_{D_p} Modified Newtonian
1.99	0.252	0.17	0.7888	0.8279
3.00	0.111	0.35	0.8480	0.8779
4.03	0.0620	0.44	0.8712	0.8968
5.06	0.0392	0.51	0.8768	0.9046
6.03	0.0275	0.37	0.8864	0.9091
8.10	0.0152	0.22	0.9000	0.9139

TABLE 4
EXPERIMENTAL SHOCK WAVE SHAPE COORDINATES

M_∞ = 1.99		M_∞ = 3		M_∞ = 4.03		M_∞ = 5.06		M_∞ = 6.03	
x/d	R/d	x/d	R/d	x/d	R/d	x/d	R/d	x/d	R/d
0	0.505		0.352	0	0.315	0	0.268	0	0.166
0.085	0.659	0.085	0.486	0.085	0.468	0.085	0.427	0.085	0.378
0.170	0.811	0.170	0.607	0.170	0.573	0.170	0.516	0.170	0.505
0.254	0.911	0.254	0.698	0.254	0.667	0.254	0.602	0.254	0.580
0.339	1.014	0.339	0.785	0.339	0.724	0.339	0.661	0.339	0.652
0.424	1.117	0.424	0.855	0.424	0.809	0.424	0.729	0.424	0.726
0.509	1.207	0.509	0.921	0.509	0.850	0.509	0.791	0.509	0.796
0.593	1.299	0.593	0.988	0.593	0.917	0.593	0.857	0.678	0.883
0.678	1.396	0.678	1.055	0.678	0.987	0.678	0.909	0.848	0.971
0.763	1.477	0.763	1.116	0.848	1.081	0.848	0.996	1.017	1.065
0.848	1.559	0.848	1.179	1.017	1.168	1.017	1.091	1.187	1.135
0.932	1.629	0.932	1.230	1.187	1.261	1.187	1.186	1.356	1.198
1.017	1.721	1.017	1.286	1.356	1.342	1.356	1.250	1.526	1.261
1.102	1.802	1.102	1.339	1.526	1.440	1.526	1.323	1.695	1.333
1.187	1.870	1.187	1.393	1.695	1.513	1.695	1.407	1.865	1.405
1.272	1.946	1.272	1.446	1.865	1.586	1.865	1.482	2.034	1.458
1.356	2.014	1.356	1.498	2.034	1.676	2.034	1.530	2.204	1.532
1.526	2.144	1.526	1.593	2.204	1.748	2.204	1.589	2.373	1.588
1.695	2.288	1.695	1.696	2.373	1.818	2.313	1.654	2.543	1.663
1.865	2.432	1.865	1.784	2.543	1.883	2.543	1.730	2.882	1.786
2.034	2.577	2.034	1.791	2.882	2.022	2.882	1.839	3.221	1.870
2.204	2.695	2.204	1.963	3.221	2.151	3.221	1.950	3.560	1.982
2.373	2.829	2.373	2.068	3.560	2.286	3.560	2.063	3.899	2.085
2.543	2.955	2.713	2.232	3.899	2.414	3.899	2.182	4.238	2.174
2.713	3.081	3.052	2.389	4.238	2.531	4.238	2.282	4.577	2.256
2.882	3.189	3.391	2.554	4.577	2.649	4.577	2.375	4.916	2.328
3.052	3.231	3.730	2.700	4.916	2.775	4.916	2.484	5.256	2.432
3.221	3.432	4.069	2.835	5.256	2.883	5.256	2.589	5.595	2.521
		4.408	2.998	5.595	3.009	5.595	2.714	5.934	2.595
		4.747	3.143	5.934	3.117	5.934	2.804	6.273	2.694
		5.086	3.300	6.273	3.240	6.273	2.911	6.612	2.796
		5.425	3.448	6.612	3.351	6.612	3.018	6.751	2.829
				6.751	3.405	6.751	3.071		

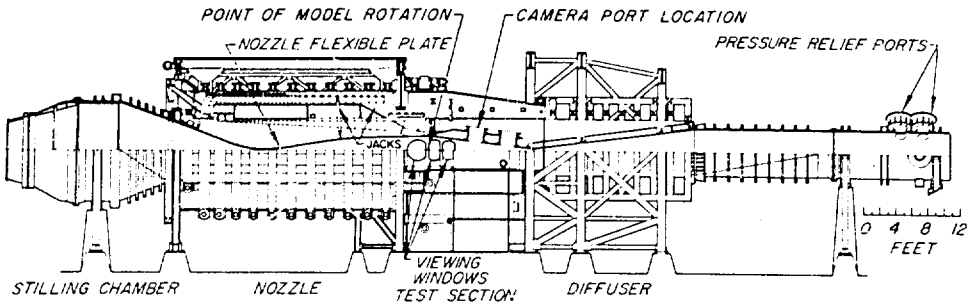

Assembly

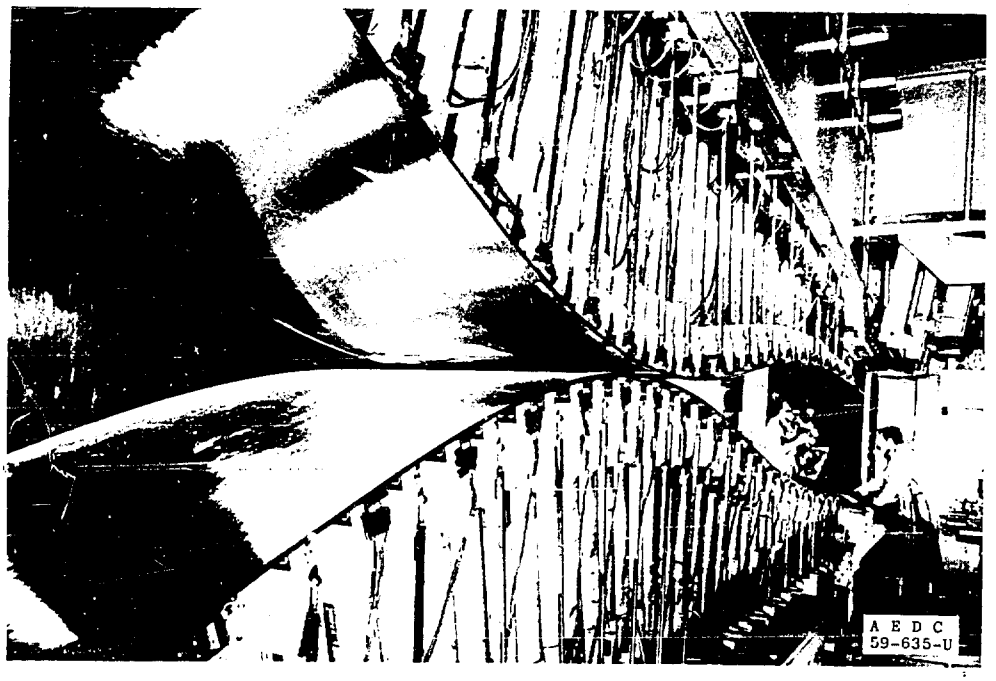

Nozzle and Test Section

Fig. 1 Tunnel A, a 40 by 40-in. Supersonic Wind Tunnel

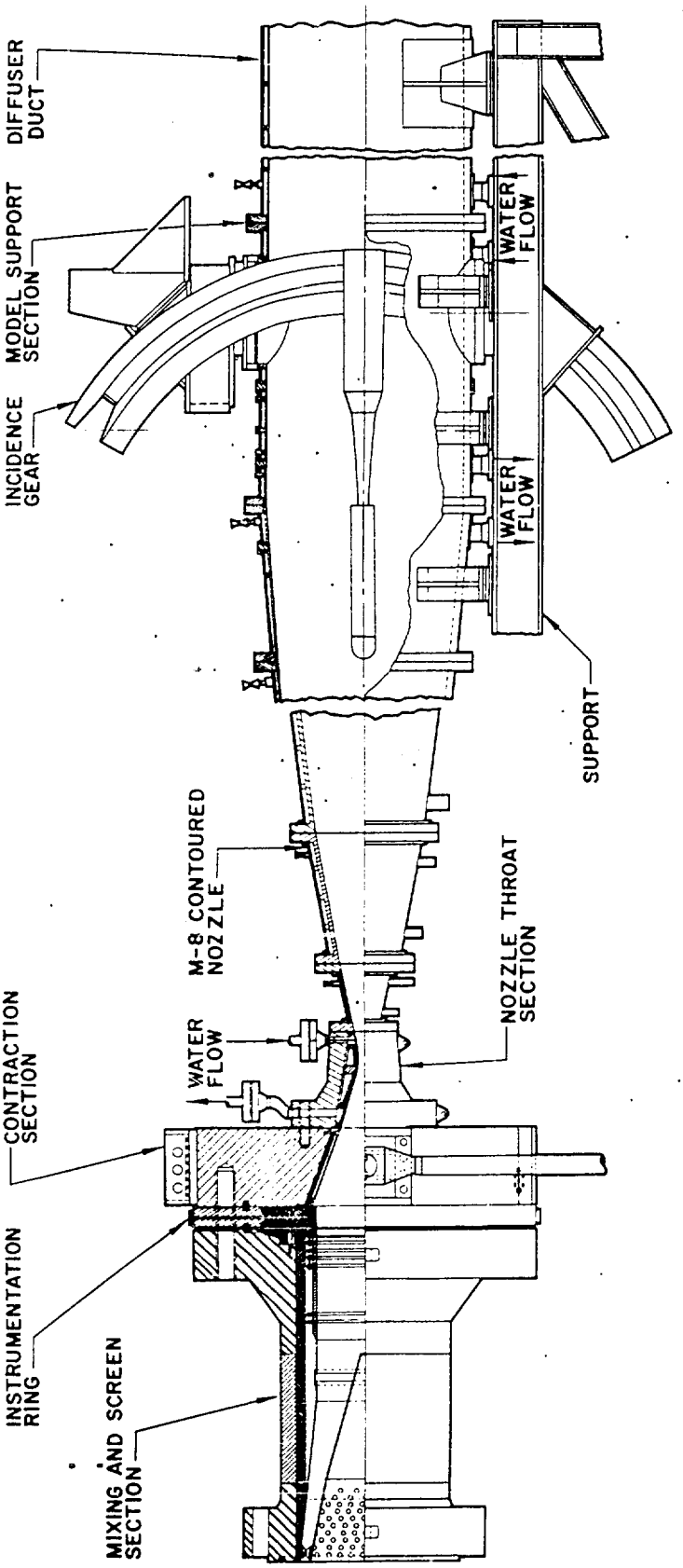

Fig. 2 Tunnel B, a 50-in.-Diam Hypersonic Wind Tunnel

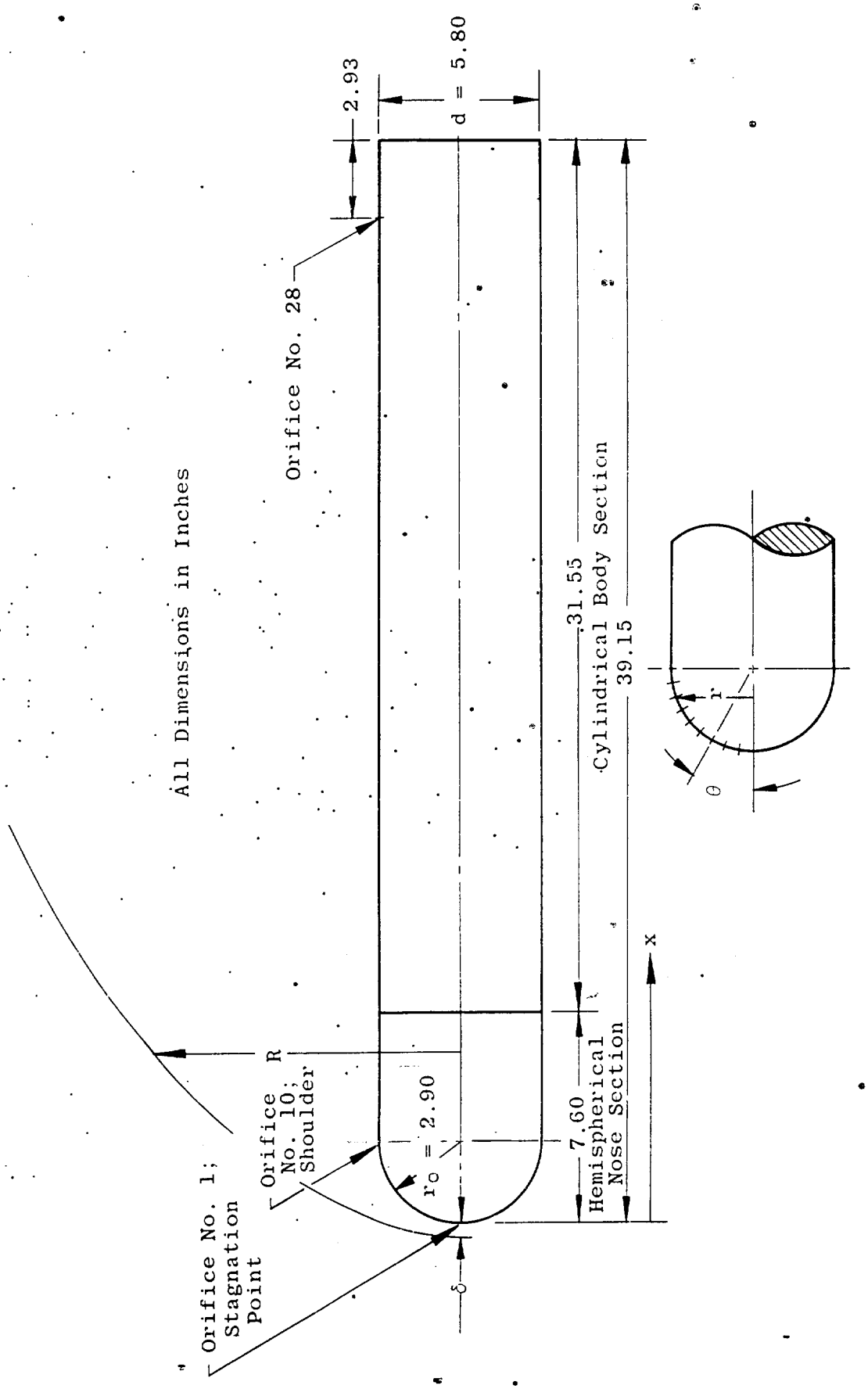

Fig. 3 Model Geometry

Fig. 4 AGARD Model E

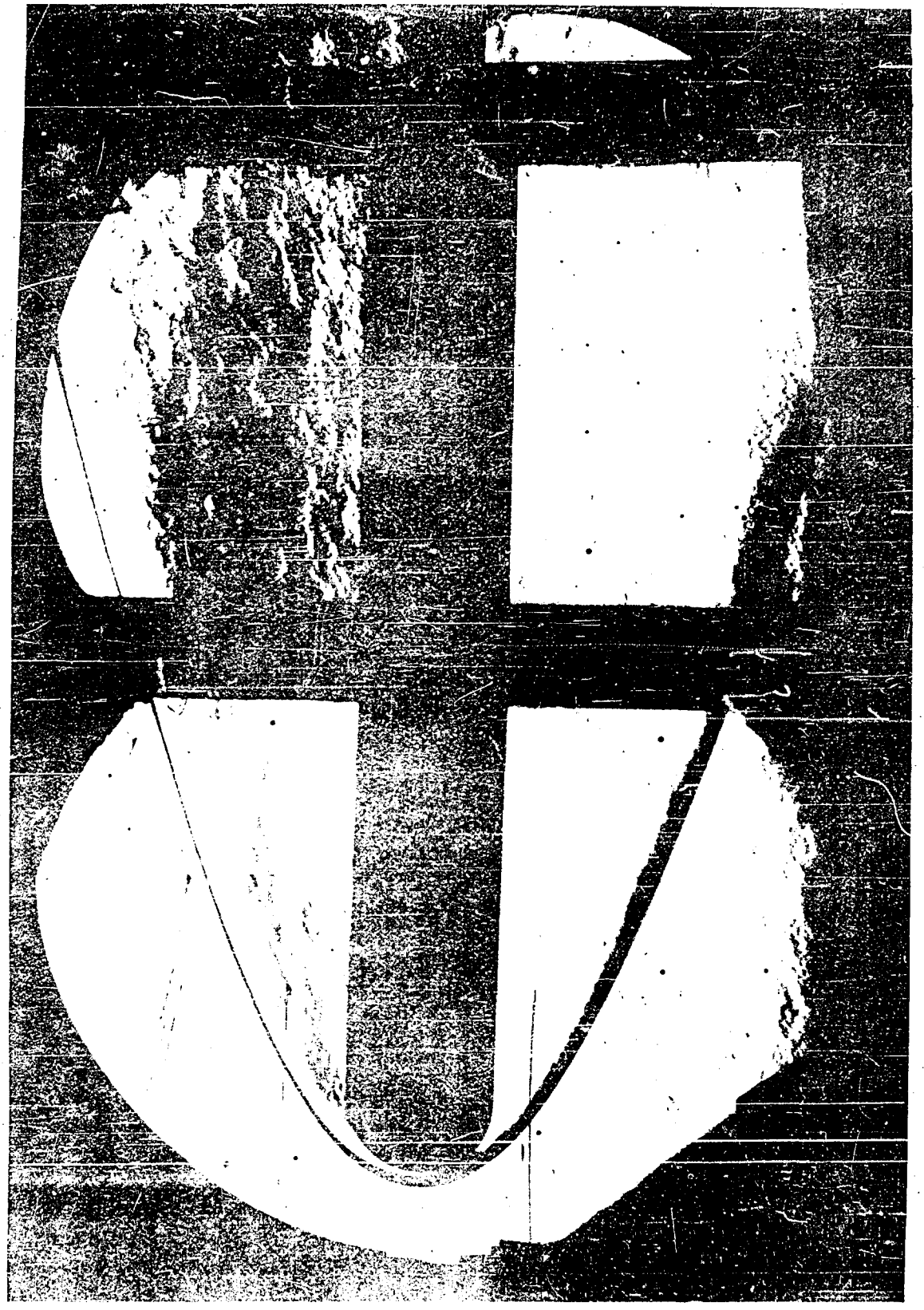

a. M_∞ = 5.06, Re/in. = 0.51 x 10^6

Fig. 5 Selected Flow Patterns

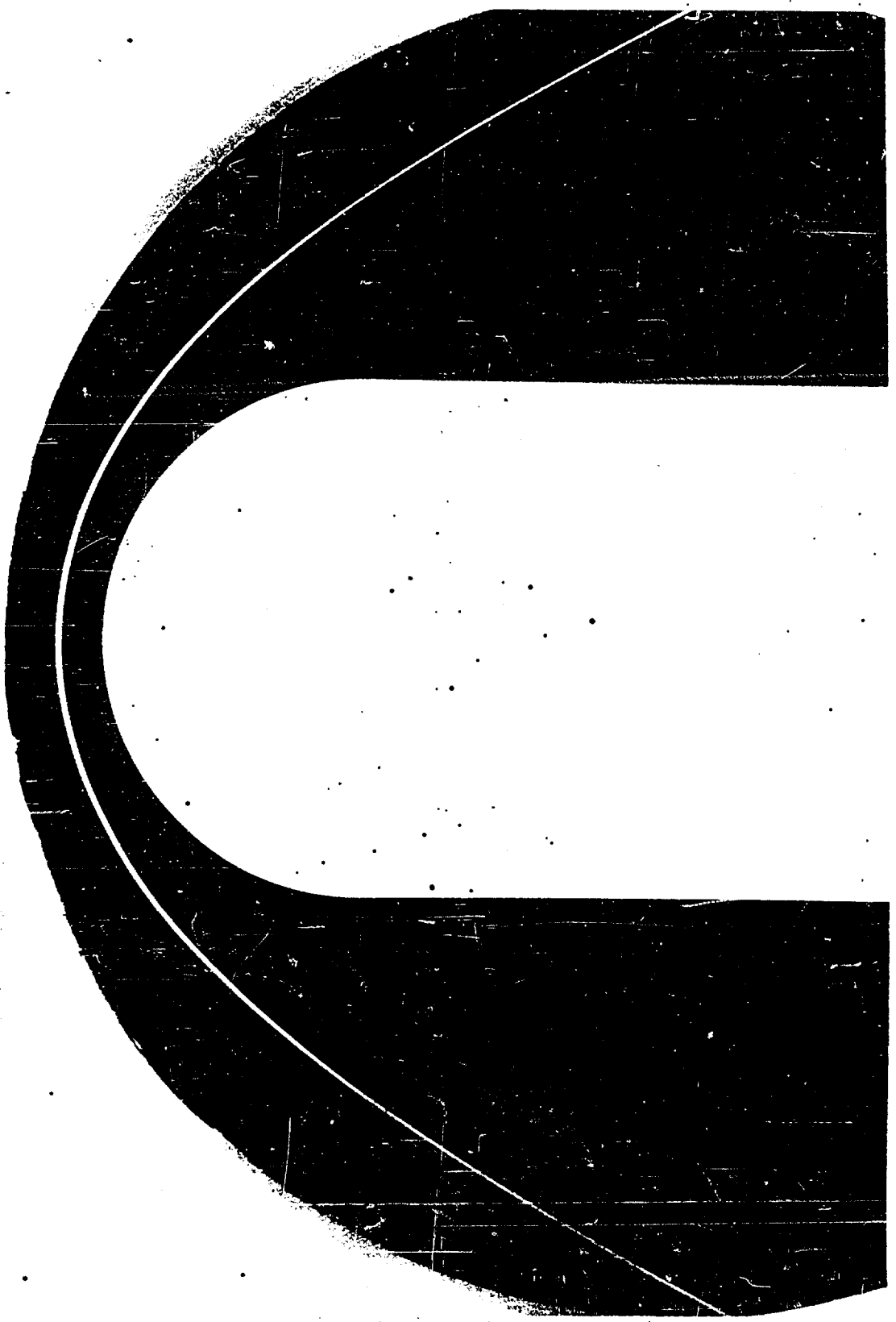

b. M_∞ = 4.03, Re/in. = 0.44 x 10^6

Fig. 5 Concluded

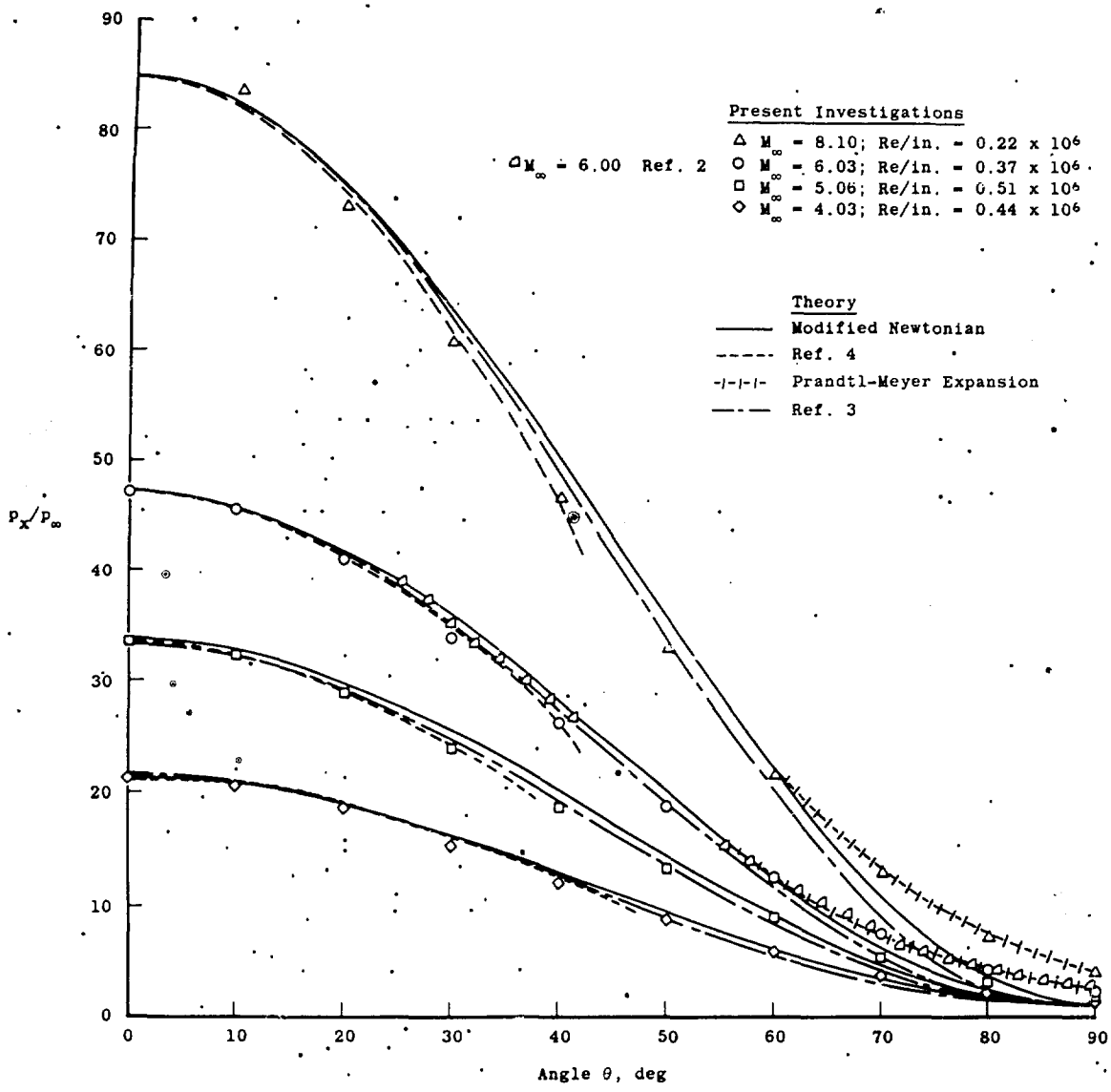

Fig. 6 A Comparison of Experimental Pressure Distributions over the Hemispherical Nose with Theoretical Predictions

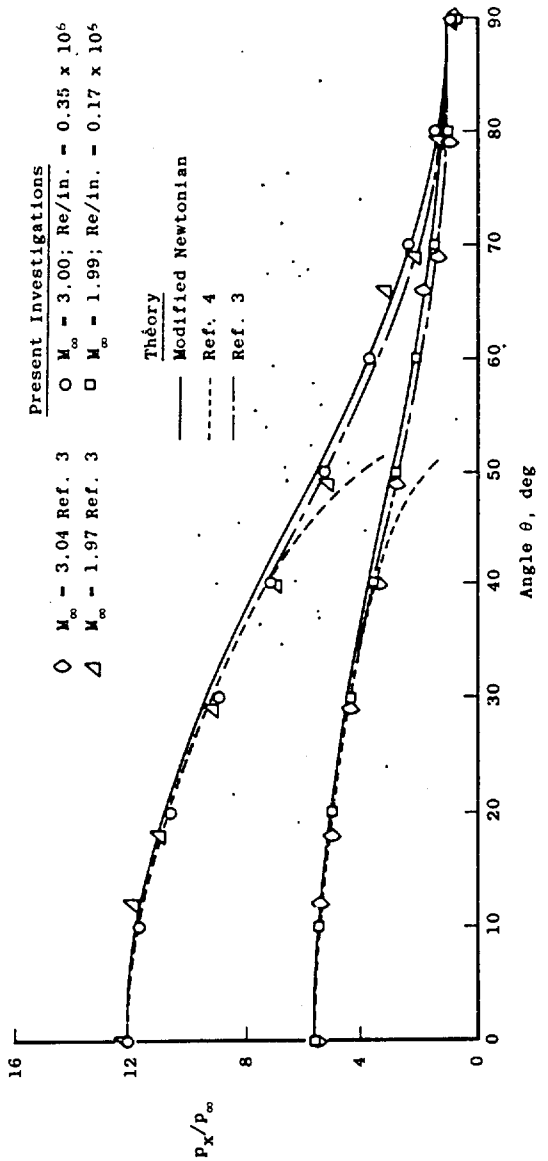

Fig. 6 Concluded

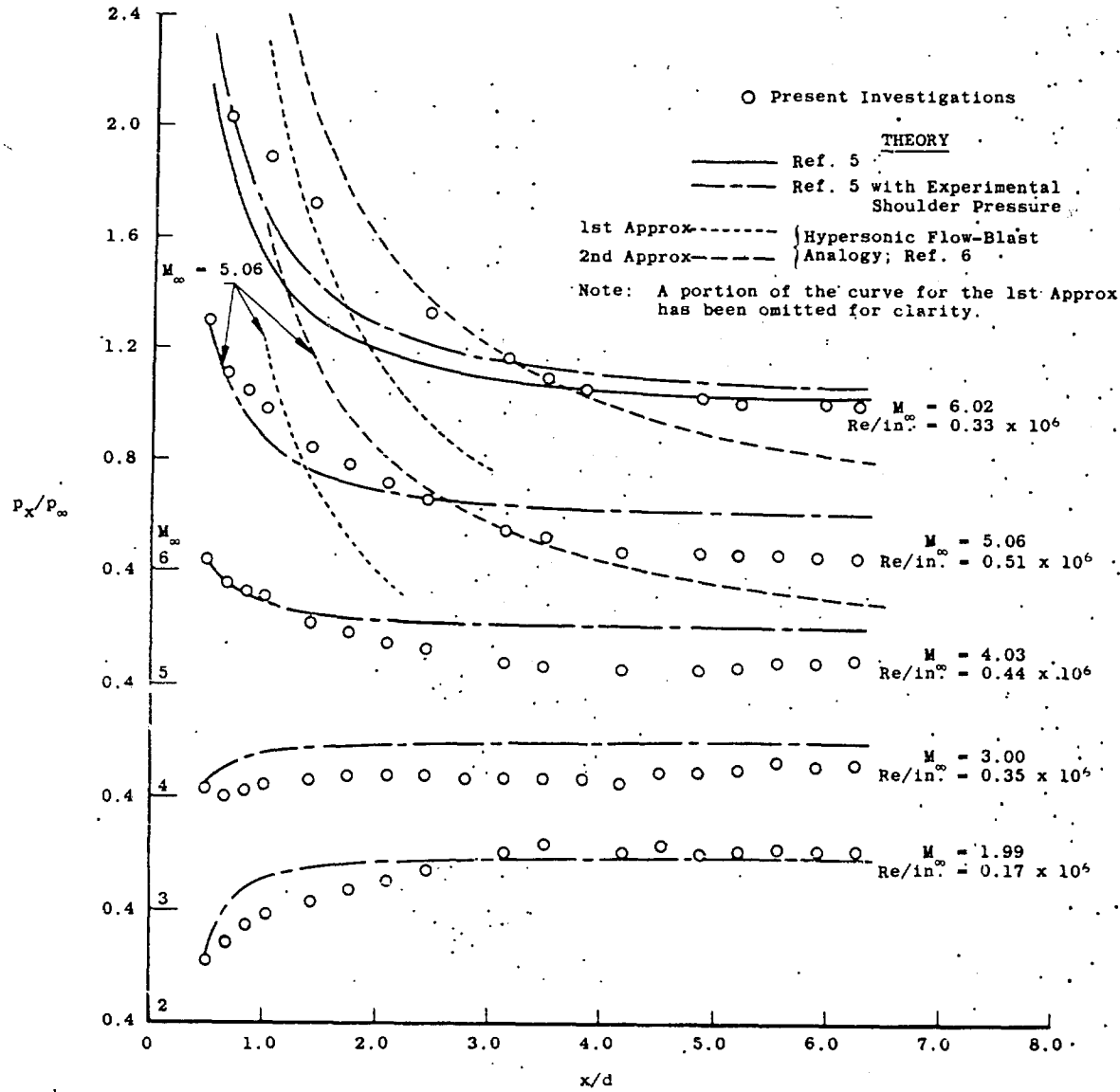

Fig. 7 Experimental and Theoretical Pressure Distributions along Cylindrical Body

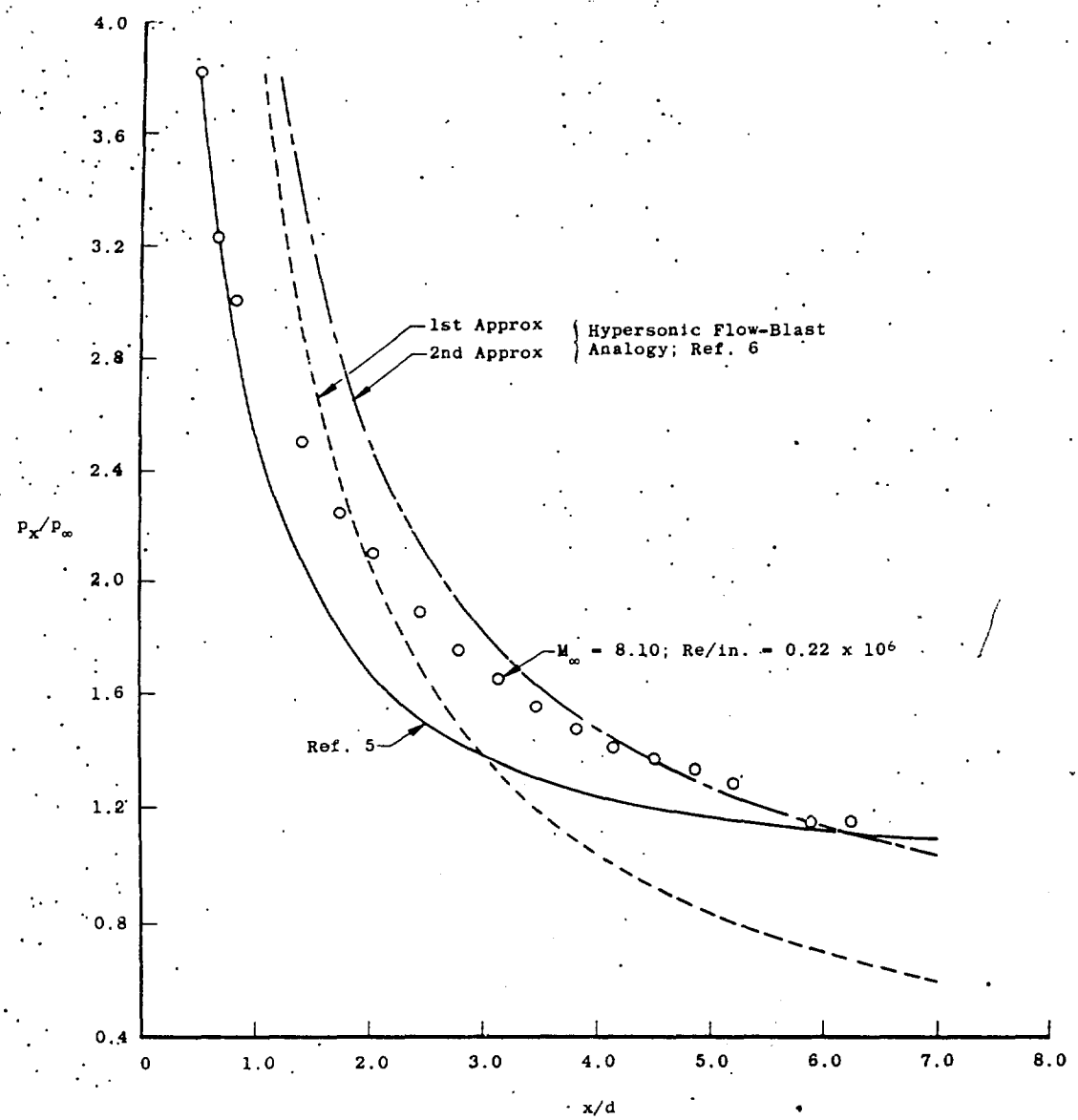

Fig. 7 Concluded

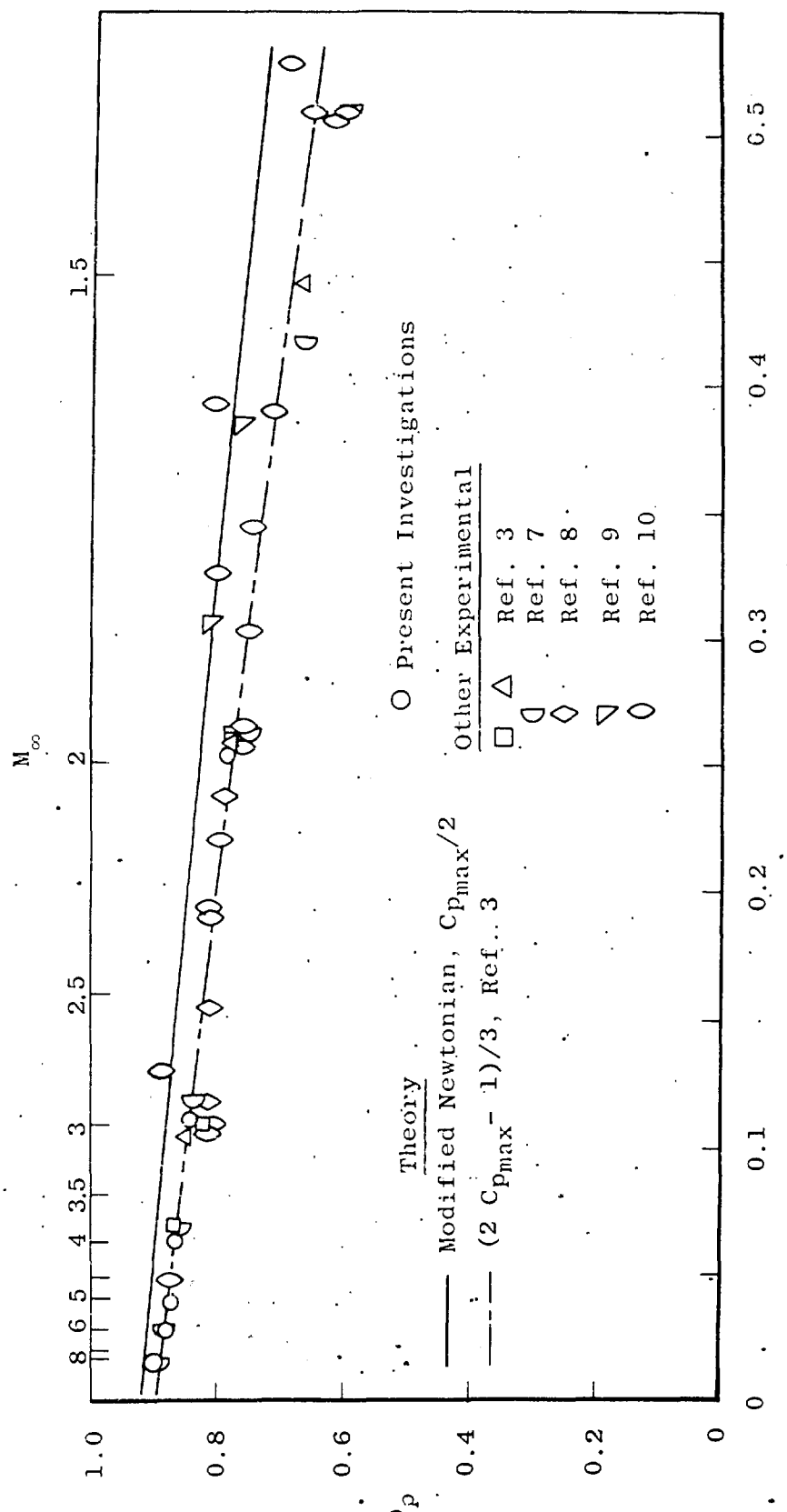

Fig. 8 Experimental Pressure Drag Coefficients Compared with Theoretical Predictions

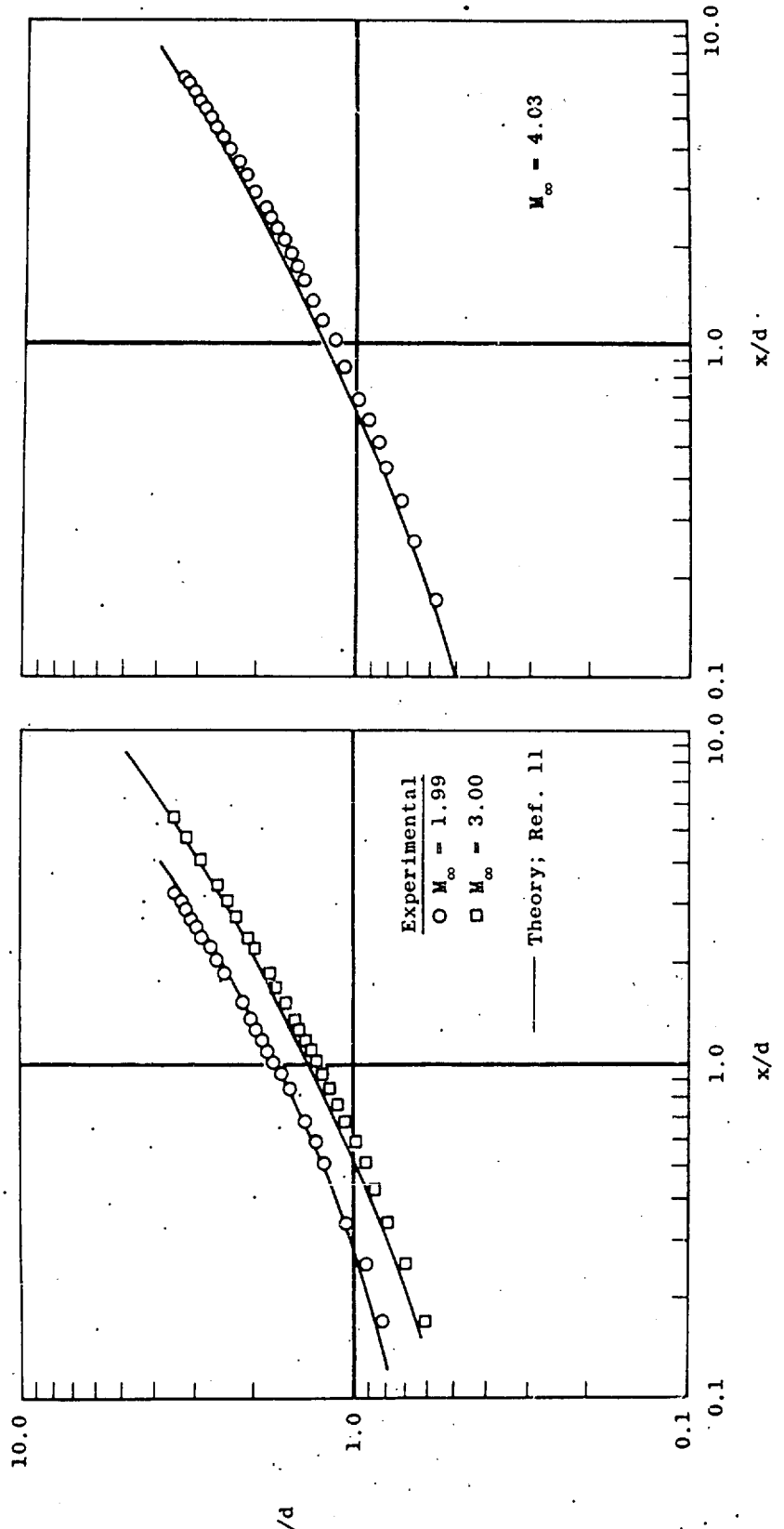

Fig. 9 A Comparison of Experimental and Theoretical Shock Wave Shapes

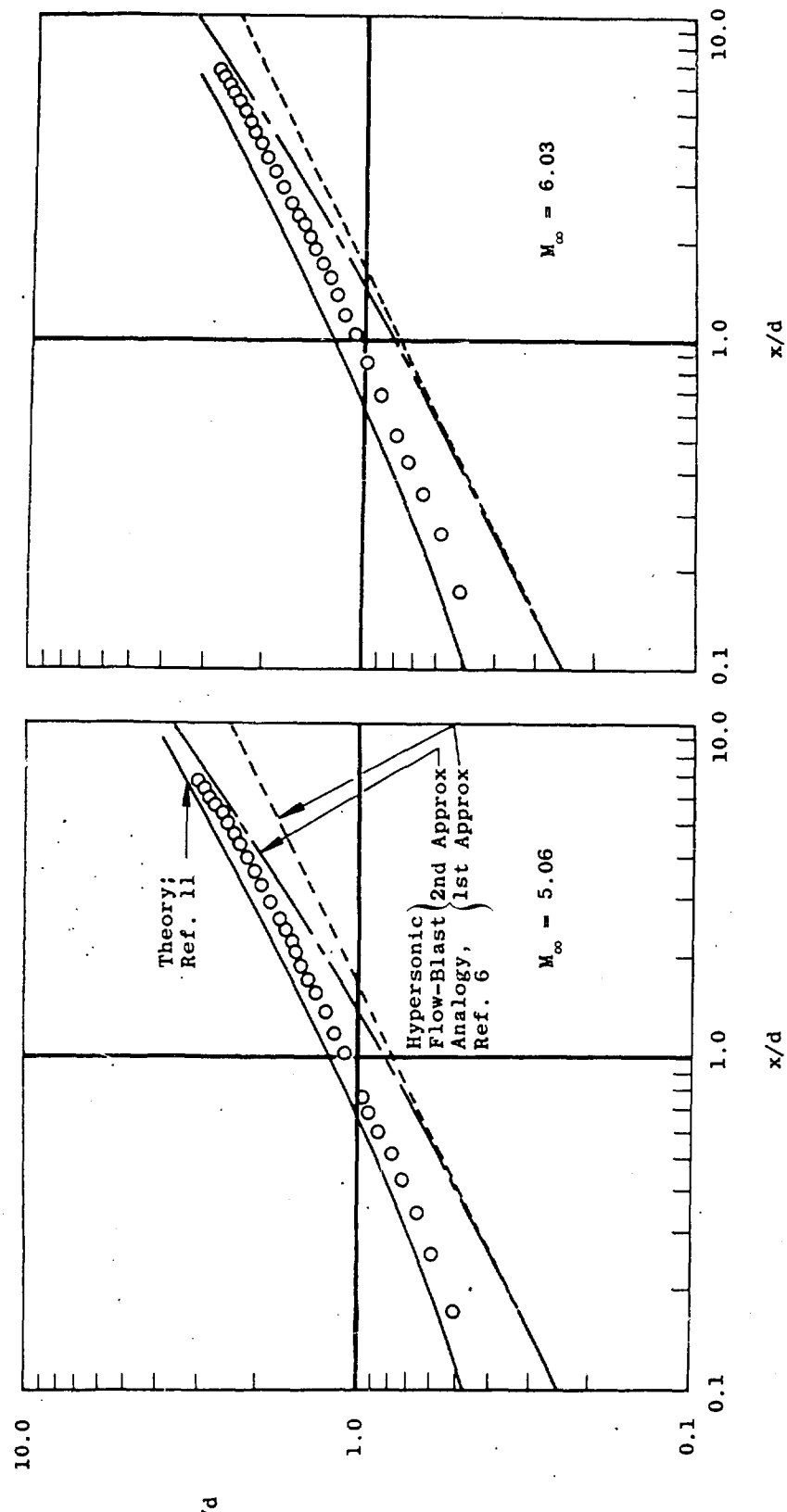

Fig. 9 Concluded

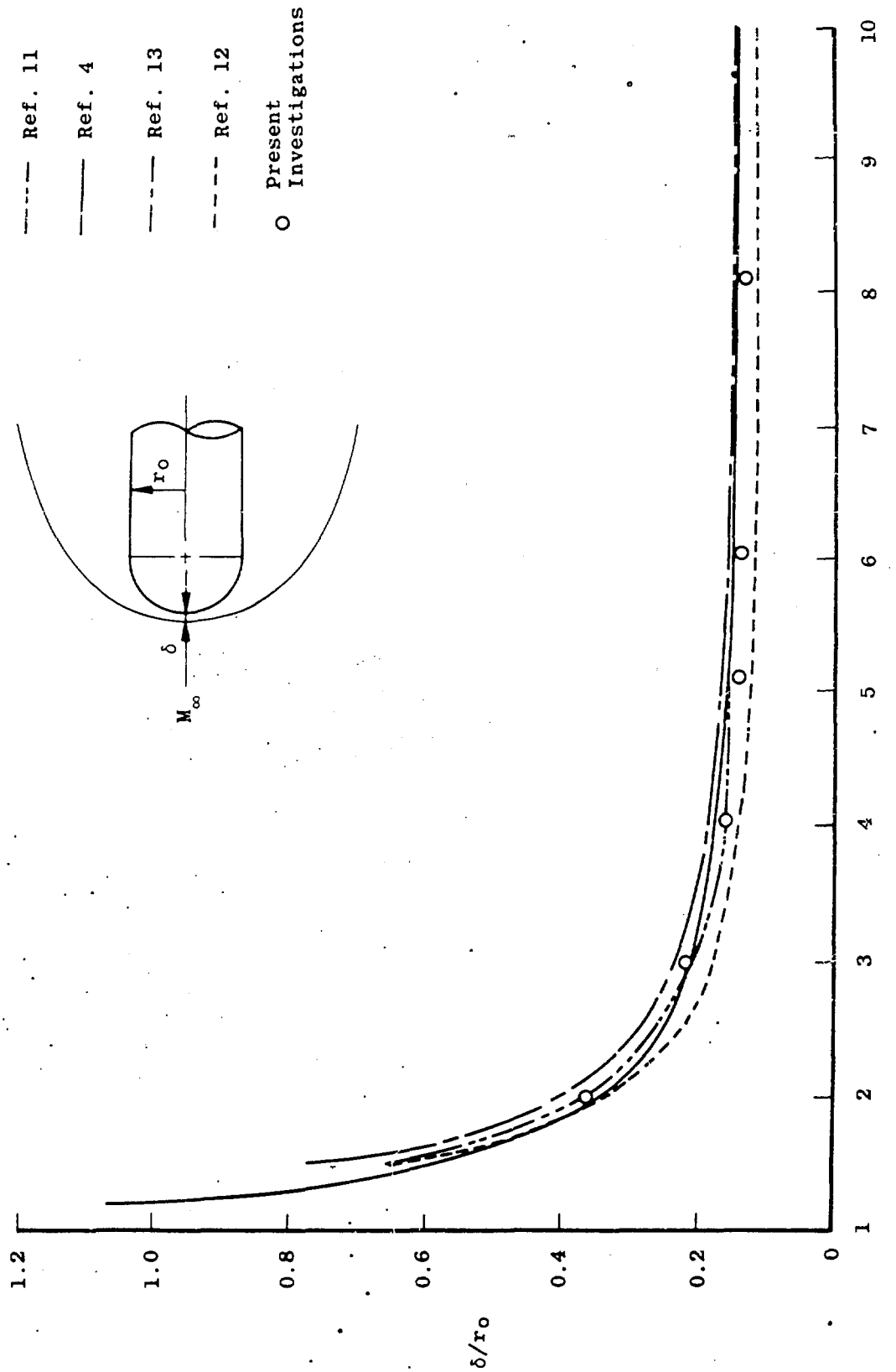

Fig. 10 Experimental Shock Wave Detachment Distances Compared with Theoretical Predictions

Cut on broken line

AEDC-TN-61-96

Arnold Engineering Development Center, ARO, Inc., Arnold Air Force Station, Tennessee
PRESSURE DISTRIBUTIONS ON A HEMISPHERE CYLINDER AT SUPERSONIC AND HYPERSONIC MACH NUMBERS by A. L. Baer. August 1961. 34 pp. (ARO Project No. 300116) (AEDC-TN-61-96) (Contract No. AF 40(600)-800 S/A 24(61-73)). Unclassified

13 references

Pressure distribution tests at supersonic and hypersonic speeds were conducted in the von Karman Gas Dynamics Facility (VKF), Arnold Center, Air Force Systems Command on AGARD Model E, a hemisphere cylinder configuration. Various experimental data concerning the aerodynamic characteristics of blunt nosed bodies are available; however, relatively few sources present findings over a wide Mach number range. The present investigations, stimulated by the need for applicable experimental data to compare with the predictions of various theories, were (over)

UNCLASSIFIED

1. Blunt-nose bodies--Pressure distribution
2. Blunt-nose bodies--Hypersonic flow
3. Blunt-nose bodies--Supersonic flow
I. Baer, A. L.

UNCLASSIFIED

AEDC-TN-61-96

Arnold Engineering Development Center, ARO, Inc., Arnold Air Force Station, Tennessee
PRESSURE DISTRIBUTIONS ON A HEMISPHERE CYLINDER AT SUPERSONIC AND HYPERSONIC MACH NUMBERS by A. L. Baer. August 1961. 34 pp. (ARO Project No. 300116) (AEDC-TN-61-96) (Contract No. AF 40(600)-800 S/A 24(61-73)). Unclassified

13 references

Pressure distribution tests at supersonic and hypersonic speeds were conducted in the von Karman Gas Dynamics Facility (VKF), Arnold Center, Air Force Systems Command on AGARD Model E, a hemisphere cylinder configuration. Various experimental data concerning the aerodynamic characteristics of blunt nosed bodies are available; however, relatively few sources present findings over a wide Mach number range. The present investigations, stimulated by the need for applicable experimental data to compare with the predictions of various theories, were (over)

UNCLASSIFIED

1. Blunt-nose bodies--Pressure distribution
2. Blunt-nose bodies--Hypersonic flow
3. Blunt-nose bodies--Supersonic flow
I. Baer, A. L.

UNCLASSIFIED

AEDC-TN-61-96

Arnold Engineering Development Center, ARO, Inc., Arnold Air Force Station, Tennessee
PRESSURE DISTRIBUTIONS ON A HEMISPHERE CYLINDER AT SUPERSONIC AND HYPERSONIC MACH NUMBERS by A. L. Baer. August 1961. 34 pp. (ARO Project No. 300116) (AEDC-TN-61-96) (Contract No. AF 40(600)-800 S/A 24(61-73)). Unclassified

13 references

Pressure distribution tests at supersonic and hypersonic speeds were conducted in the von Karman Gas Dynamics Facility (VKF), Arnold Center, Air Force Systems Command on AGARD Model E, a hemisphere cylinder configuration. Various experimental data concerning the aerodynamic characteristics of blunt nosed bodies are available; however, relatively few sources present findings over a wide Mach number range. The present investigations, stimulated by the need for applicable experimental data to compare with the predictions of various theories, were (over)

UNCLASSIFIED

1. Blunt-nose bodies--Pressure distribution
2. Blunt-nose bodies--Hypersonic flow
3. Blunt-nose bodies--Supersonic flow
I. Baer, A. L.

UNCLASSIFIED

AEDC-TN-61-96

Arnold Engineering Development Center, ARO, Inc., Arnold Air Force Station, Tennessee
PRESSURE DISTRIBUTIONS ON A HEMISPHERE CYLINDER AT SUPERSONIC AND HYPERSONIC MACH NUMBERS by A. L. Baer. August 1961. 34 pp. (ARO Project No. 300116) (AEDC-TN-61-96) (Contract No. AF 40(600)-800 S/A 24(61-73)). Unclassified

13 references

Pressure distribution tests at supersonic and hypersonic speeds were conducted in the von Karman Gas Dynamics Facility (VKF), Arnold Center, Air Force Systems Command on AGARD Model E, a hemisphere cylinder configuration. Various experimental data concerning the aerodynamic characteristics of blunt nosed bodies are available; however, relatively few sources present findings over a wide Mach number range. The present investigations, stimulated by the need for applicable experimental data to compare with the predictions of various theories, were (over)

UNCLASSIFIED

1. Blunt-nose bodies--Pressure distribution
2. Blunt-nose bodies--Hypersonic flow
3. Blunt-nose bodies--Supersonic flow
I. Baer, A. L.

UNCLASSIFIED

AEDC-TN-61-96

conducted at Mach numbers 2 through 8 over a Reynolds number range from 0.17×10^6 to 0.51×10^6 per inch. This report presents a comparison of experimental results with available theoretical predictions of pressure distributions, pressure drag, shock wave shapes, and bow shock wave detachment distances.

UNCLASSIFIED

UNCLASSIFIED

AEDC-TN-61-96

conducted at Mach numbers 2 through 8 over a Reynolds number range from 0.17×10^6 to 0.51×10^6 per inch. This report presents a comparison of experimental results with available theoretical predictions of pressure distributions, pressure drag, shock wave shapes, and bow shock wave detachment distances.

UNCLASSIFIED

AEDC-TN-61-96

conducted at Mach numbers 2 through 8 over a Reynolds number range from 0.17×10^6 to 0.51×10^6 per inch. This report presents a comparison of experimental results with available theoretical predictions of pressure distributions, pressure drag, shock wave shapes, and bow shock wave detachment distances.

UNCLASSIFIED

AEDC TN-61-96

conducted at Mach numbers 2 through 8 over a Reynolds number range from 0.17×10^6 to 0.51×10^6 per inch. This report presents a comparison of experimental results with available theoretical predictions of pressure distributions, pressure drag, shock wave shapes, and bow shock wave detachment distances.

UNCLASSIFIED

Cut on broken line

AEDC-TN-61-96

Arnold Engineering Development Center, ARO, Inc., Arnold Air Force Station, Tennessee
PRESSURE DISTRIBUTIONS ON A HEMISPHERE CYLINDER AT SUPERSONIC AND HYPERSONIC MACH NUMBERS by A. L. Baer. August 1961. 34 pp. (ARO Project No. 300116) (AEDC-TN-61-96) (Contract No. AF 40(600)-800 S/A 24(61-73)). Unclassified

13 references

Pressure distribution tests at supersonic and hypersonic speeds were conducted in the von Karman Gas Dynamics Facility (VKF), Arnold Center, Air Force Systems Command on AGARD Model E, a hemisphere cylinder configuration. Various experimental data concerning the aerodynamic characteristics of blunt nosed bodies are available; however, relatively few sources present findings over a wide Mach number range. The present investigations, stimulated by the need for applicable experimental data to compare with the predictions of various theories, were (over)

UNCLASSIFIED

1. Blunt-nose bodies--Pressure distribution
2. Blunt-nose bodies--Hypersonic flow
3. Blunt-nose bodies--Supersonic flow
I. Baer, A. L.

UNCLASSIFIED

AEDC-TN-61-96

Arnold Engineering Development Center, ARO, Inc., Arnold Air Force Station, Tennessee
PRESSURE DISTRIBUTIONS ON A HEMISPHERE CYLINDER AT SUPERSONIC AND HYPERSONIC MACH NUMBERS by A. L. Baer. August 1961. 34 pp. (ARO Project No. 300116) (AEDC-TN-61-96) (Contract No. AF 40(600)-800 S/A 24(61-73)). Unclassified

13 references

Pressure distribution tests at supersonic and hypersonic speeds were conducted in the von Karman Gas Dynamics Facility (VKF), Arnold Center, Air Force Systems Command on AGARD Model E, a hemisphere cylinder configuration. Various experimental data concerning the aerodynamic characteristics of blunt nosed bodies are available; however, relatively few sources present findings over a wide Mach number range. The present investigations, stimulated by the need for applicable experimental data to compare with the predictions of various theories, were (over)

UNCLASSIFIED

1. Blunt-nose bodies--Pressure distribution
2. Blunt-nose bodies--Hypersonic flow
3. Blunt-nose bodies--Supersonic flow
I. Baer, A. L.

UNCLASSIFIED

AEDC-TN-61-96

Arnold Engineering Development Center, ARO, Inc., Arnold Air Force Station, Tennessee
PRESSURE DISTRIBUTIONS ON A HEMISPHERE CYLINDER AT SUPERSONIC AND HYPERSONIC MACH NUMBERS by A. L. Baer. August 1961. 34 pp. (ARO Project No. 300116) (AEDC-TN-61-96) (Contract No. AF 40(600)-800 S/A 24(61-73)). Unclassified

13 references

Pressure distribution tests at supersonic and hypersonic speeds were conducted in the von Karman Gas Dynamics Facility (VKF), Arnold Center, Air Force Systems Command on AGARD Model E, a hemisphere cylinder configuration. Various experimental data concerning the aerodynamic characteristics of blunt nosed bodies are available; however, relatively few sources present findings over a wide Mach number range. The present investigations, stimulated by the need for applicable experimental data to compare with the predictions of various theories, were (over)

UNCLASSIFIED

1. Blunt-nose bodies--Pressure distribution
2. Blunt-nose bodies--Hypersonic flow
3. Blunt-nose bodies--Supersonic flow
I. Baer, A. L.

UNCLASSIFIED

AEDC-TN-61-96

Arnold Engineering Development Center, ARO, Inc., Arnold Air Force Station, Tennessee
PRESSURE DISTRIBUTIONS ON A HEMISPHERE CYLINDER AT SUPERSONIC AND HYPERSONIC MACH NUMBERS by A. L. Baer. August 1961. 34 pp. (ARO Project No. 300116) (AEDC-TN-61-96) (Contract No. AF 40(600)-800 S/A 24(61-73)). Unclassified

13 references

Pressure distribution tests at supersonic and hypersonic speeds were conducted in the von Karman Gas Dynamics Facility (VKF), Arnold Center, Air Force Systems Command on AGARD Model E, a hemisphere cylinder configuration. Various experimental data concerning the aerodynamic characteristics of blunt nosed bodies are available; however, relatively few sources present findings over a wide Mach number range. The present investigations, stimulated by the need for applicable experimental data to compare with the predictions of various theories, were (over)

UNCLASSIFIED

1. Blunt-nose bodies--Pressure distribution
2. Blunt-nose bodies--Hypersonic flow
3. Blunt-nose bodies--Supersonic flow
I. Baer, A. L.

UNCLASSIFIED

AEDC-TN-61-96

conducted at Mach numbers 2 through 8 over a Reynolds number range from 0.17×10^6 to 0.51×10^6 per inch. This report presents a comparison of experimental results with available theoretical predictions of pressure distributions, pressure drag, shock wave shapes, and bow shock wave detachment distances.

UNCLASSIFIED

UNCLASSIFIED

AEDC-TN-61-96

conducted at Mach numbers 2 through 8 over a Reynolds number range from 0.17×10^6 to 0.51×10^6 per inch. This report presents a comparison of experimental results with available theoretical predictions of pressure distributions, pressure drag, shock wave shapes, and bow shock wave detachment distances.

UNCLASSIFIED

UNCLASSIFIED

AEDC-TN-61-96

conducted at Mach numbers 2 through 8 over a Reynolds number range from 0.17×10^6 to 0.51×10^6 per inch. This report presents a comparison of experimental results with available theoretical predictions of pressure distributions, pressure drag, shock wave shapes, and bow shock wave detachment distances.

UNCLASSIFIED

UNCLASSIFIED

AEDC-TN-61-96

conducted at Mach numbers 2 through 8 over a Reynolds number range from 0.17×10^6 to 0.51×10^6 per inch. This report presents a comparison of experimental results with available theoretical predictions of pressure distributions, pressure drag, shock wave shapes, and bow shock wave detachment distances.

UNCLASSIFIED

UNCLASSIFIED

Cut on broken line

AEDC-TN-61-96

Arnold Engineering Development Center, ARO, Inc., Arnold Air Force Station, Tennessee
PRESSURE DISTRIBUTIONS ON A HEMISPHERE CYLINDER AT SUPERSONIC AND HYPERSONIC MACH NUMBERS by A. L. Baer. August 1961. 34 pp. (ARO Project No. 300116) (AEDC-TN-61-96) (Contract No. AF 40(600)-800 S/A 24(61-73)). Unclassified

13 references

Pressure distribution tests at supersonic and hypersonic speeds were conducted in the von Karman Gas Dynamics Facility (VKF), Arnold Center, Air Force Systems Command on AGARD Model E, a hemisphere cylinder configuration. Various experimental data concerning the aerodynamic characteristics of blunt nosed bodies are available, however, relatively few sources present findings over a wide Mach number range. The present investigations, stimulated by the need for applicable experimental data to compare with the predictions of various theories, were
(over)

UNCLASSIFIED

1. Blunt-nose bodies--Pressure distribution
2. Blunt-nose bodies--Hypersonic flow
3. Blunt-nose bodies--Supersonic flow
I. Baer, A. L.

UNCLASSIFIED

AEDC-TN-61-96

Arnold Engineering Development Center, ARO, Inc., Arnold Air Force Station, Tennessee
PRESSURE DISTRIBUTIONS ON A HEMISPHERE CYLINDER AT SUPERSONIC AND HYPERSONIC MACH NUMBERS by A. L. Baer. August 1961. 34 pp. (ARO Project No. 300116) (AEDC-TN-61-96) (Contract No. AF 40(600)-800 S/A 24(61-73)). Unclassified

13 references

Pressure distribution tests at supersonic and hypersonic speeds were conducted in the von Karman Gas Dynamics Facility (VKF), Arnold Center, Air Force Systems Command on AGARD Model E, a hemisphere cylinder configuration. Various experimental data concerning the aerodynamic characteristics of blunt nosed bodies are available, however, relatively few sources present findings over a wide Mach number range. The present investigations, stimulated by the need for applicable experimental data to compare with the predictions of various theories, were
(over)

UNCLASSIFIED

1. Blunt-nose bodies--Pressure distribution
2. Blunt-nose bodies--Hypersonic flow
3. Blunt-nose bodies--Supersonic flow
I. Baer, A. L.

UNCLASSIFIED

AEDC-TN-61-96

Arnold Engineering Development Center, ARO, Inc., Arnold Air Force Station, Tennessee
PRESSURE DISTRIBUTIONS ON A HEMISPHERE CYLINDER AT SUPERSONIC AND HYPERSONIC MACH NUMBERS by A. L. Baer. August 1961. 34 pp. (ARO Project No. 300116) (AEDC-TN-61-96) (Contract No. AF 40(600)-800 S/A 24(61-73)). Unclassified

13 references

Pressure distribution tests at supersonic and hypersonic speeds were conducted in the von Karman Gas Dynamics Facility (VKF), Arnold Center, Air Force Systems Command on AGARD Model E, a hemisphere cylinder configuration. Various experimental data concerning the aerodynamic characteristics of blunt nosed bodies are available; however, relatively few sources present findings over a wide Mach number range. The present investigations, stimulated by the need for applicable experimental data to compare with the predictions of various theories, were
(over)

UNCLASSIFIED

1. Blunt-nose bodies--Pressure distribution
2. Blunt-nose bodies--Hypersonic flow
3. Blunt-nose bodies--Supersonic flow
I. Baer, A. L.

UNCLASSIFIED

AEDC-TN-61-96

Arnold Engineering Development Center, ARO, Inc., Arnold Air Force Station, Tennessee
PRESSURE DISTRIBUTIONS ON A HEMISPHERE CYLINDER AT SUPERSONIC AND HYPERSONIC MACH NUMBERS by A. L. Baer. August 1961. 34 pp. (ARO Project No. 300116) (AEDC-TN-61-96) (Contract No. AF 40(600)-800 S/A 24(61-73)). Unclassified

13 references

Pressure distribution tests at supersonic and hypersonic speeds were conducted in the von Karman Gas Dynamics Facility (VKF), Arnold Center, Air Force Systems Command on AGARD Model E, a hemisphere cylinder configuration. Various experimental data concerning the aerodynamic characteristics of blunt nosed bodies are available; however, relatively few sources present findings over a wide Mach number range. The present investigations, stimulated by the need for applicable experimental data to compare with the predictions of various theories, were
(over)

UNCLASSIFIED

1. Blunt-nose bodies--Pressure distribution
2. Blunt-nose bodies--Hypersonic flow
3. Blunt-nose bodies--Supersonic flow
I. Baer, A. L.

UNCLASSIFIED

AEDC-TN-61-96

conducted at Mach numbers 2 through 8 over a Reynolds number range from 0.17×10^6 to 0.51×10^6 per inch. This report presents a comparison of experimental results with available theoretical predictions of pressure distributions, pressure drag, shock wave shapes, and bow shock wave detachment distances.

UNCLASSIFIED

UNCLASSIFIED

AEDC-TN-61-96

conducted at Mach numbers 2 through 8 over a Reynolds number range from 0.17×10^6 to 0.51×10^6 per inch. This report presents a comparison of experimental results with available theoretical predictions of pressure distributions, pressure drag, shock wave shapes, and bow shock wave detachment distances.

UNCLASSIFIED

UNCLASSIFIED

AEDC-TN-61-96

conducted at Mach numbers 2 through 8 over a Reynolds number range from 0.17×10^6 to 0.51×10^6 per inch. This report presents a comparison of experimental results with available theoretical predictions of pressure distributions, pressure drag, shock wave shapes, and bow shock wave detachment distances.

UNCLASSIFIED

UNCLASSIFIED

AEDC-TN-61-96

conducted at Mach numbers 2 through 8 over a Reynolds number range from 0.17×10^6 to 0.51×10^6 per inch. This report presents a comparison of experimental results with available theoretical predictions of pressure distributions, pressure drag, shock wave shapes, and bow shock wave detachment distances.

UNCLASSIFIED

UNCLASSIFIED

DEPARTMENT OF THE AIR FORCE
HEADQUARTERS ARNOLD ENGINEERING DEVELOPMENT CENTER (AFMC)
ARNOLD AIR FORCE BASE TENNESSEE

MEMORANDUM FOR DTIC-OCQ 7 JUN 2002
8725 John J. Kingman Road
Fort Bel;voir VA 22060-6218
Attn: Larry Downing, 703-76-0011

FROM: AEDC/IN-STINFO
251 First Street
Arnold AFB TN 37389-2305

SUBJ: Change in Distribution Statement/Restrictions

1. The below listed Technical Report has been reviewed by the OPR and it has been determine that there are no restrictions required on this report and should be made available to the general public, Distribution Statement A:

AEDC-TN-61-96

2. Point of contact is the undersigned at DSN 340-7329 or Com 931-454-7329.

J. W. CAMPBELL
AEDC Stinfo Officer